

Valence-State Atoms in Molecules. 6. Universal Ionic–Covalent Potential Energy Curves

László von Szentpály* and Devon O. Niel Gardner

Department of Chemistry, University of the West Indies, Mona Campus, Kingston 7, Jamaica

Received: July 10, 2001

A semiempirical approach for constructing a universal ionic–covalent (UIC) potential energy curve is presented, and two related UIC functions are discussed. In the vicinity of the equilibrium bond length, the attraction between the atoms in the molecule (AIM) is modeled as purely Coulombic, $-C/R$, as implied by the asymptotic reference to the promoted valence-state energy of partially charged atoms [Gardner, D.; Szentpály, L. v. *J. Phys. Chem. A* 1999, 103, 9313]. The partial charge is calculated by electronegativity equalization. Along the dissociation coordinate R , we model the decreasing contribution of “ionic structures” as a “soft” Coulson–Fischer transition: the composite UIC function is generated by continuously reducing the weight of the valence-state potential energy function by the admixture of a modified Morse function. Average unsigned errors of 1.42% and 1.16% of D_e are obtained by comparing our five-parameter UIC and UIC $_{\alpha}$ curves with the full Rydberg–Klein–Rees, or *ab initio*, curves of 42 covalent or polar diatomic molecules (from H₂ to NaCl). The evaluation of the rotation–vibration coupling constant, α_e , requires only three parameters and yields an average unsigned error of 6.37% for 50 molecules.

1. Introduction

In the preceding paper in this series,¹ we documented the agreement between the valence-state potential energy curve (VS PEC) and experimental data of 50 diatomic molecules up to the Coulson–Fischer transition² at $R \approx 1.6R_e$. Other previous work^{3–8} defined the valence-state atoms (VSA)^{3,4,8} with their orbital electronegativity (χ_{vs} , VSEN) and chemical hardness (η_{vs}), and examined their extension to groups in molecules.⁸ A gas-phase electrophilicity index for atoms, groups, and molecules was introduced.^{7,8} The VS PEC was generated, and its universal scaling properties and transferable force constant increments were discussed.^{4–6} In this article, the range of the VS PEC is extended to $R \rightarrow \infty$ in the form of a universal ionic–covalent curve (UICC) involving the admixture of a modified Morse PEC.

One main source for PE functions is the direct (or indirect) inversion of spectroscopic data. For diatomic molecules the Rydberg–Klein–Rees (RKR) turning points are obtained by a semiclassical inversion process using the observed vibrational and rotational states,^{9,10} and the set of points $U(R_i)$ is connected by analytical potentials,^{9,11–13} truncated power series,^{14–17} or Padé approximants.¹⁸ Similarly to experiments, theoretical methods yield $U(R_i)$ data for some discrete set of internuclear distances, so that PE curves and surfaces have to be obtained by interpolation. Analytical PECs are preferable, to achieve scaling¹ and transferability of the parameters,⁶ and to gain qualitative insight that may not be obvious from the other interpolation techniques. Recent work on structure, dynamics, and thermodynamics of clusters demonstrates the usefulness of simple, analytical pair potentials, e.g., Morse potential, even for very large systems containing 150 atoms.¹⁹

With the notable exceptions of a few semiempirical forms, e.g., ionic PECs,^{20,21} the simple-bond-charge model,²² and

Nalewajski's functions,²³ most analytical potentials, such as the Morse,²⁴ Rydberg⁹ with its extensions,¹³ and the suite of Varshni PECs¹¹ have been purely empirical and characterized as lacking physical interpretability.¹² Semiempirical functions, to which the VS PEC belongs, use limited inputs of theoretical concepts with results from calculations of average accuracy for their construction. Such simple models have the advantage of appealing to physicochemical intuition, may require no more than a pen and paper, and are capable of making useful predictions to within a few percent of the RKR data. It is believed that analytical functions with the highest degree of transferability are semiempirical and are based on sound quantum mechanical bonding principles.^{6,25}

2. The Quest for the Universal Potential

The search for the universal PEC aims at the comparative study of reduced PECs of different molecules in a unified scheme. The postulated existence of a universal PE function, capable of predicting RKR data and spectroscopic constants for all diatomic molecules, has been the subject of numerous investigations spread over most of the 20th century.^{1,4–6,9–13,23–34} The idea is analogous to that of the reduced equation of states for all real gases, and the universal PEC has been occasionally called the “Holy Grail of spectroscopy”.^{30,34} The elusiveness of such a function led Varshni to conclude, “it is not possible to find three constant “universal” potential energy functions”.¹¹ Graves and Parr^{29a} later clarified this statement with respect to the more stringent requirement of universal linear scaling of three-parameter potentials. Using different approaches and a larger number of parameters, Jenč,²⁷ Ferrante et al.,²⁸ Tellinghuisen et al.,³⁰ and Zavitsas³³ independently showed that a generalized scaling into a single reduced PEC is feasible for most systems. Exceptions, such as the alkali metal halides in Zavitsas' treatment, confirm the rule;³³ this led us to revisit the universal PEC problem.⁴

The degree to which potential energy functions may be considered universal is still an unresolved subject. A commonly

* To whom correspondence should be addressed at Institut für Theoretische Chemie, Universität Stuttgart, Pfaffenwaldring 55, D-70569 Stuttgart, Germany.

accepted “measure” seems to be the extent and quality of universal scaling of the available experimental curves.^{1,26–33} This relates to assessing the ability of a function to fulfill spectroscopic performance tests for a large variety of bonds.^{4,11,12} Such universality criteria are (i) the ability of the function to predict spectroscopic constants to which it has not been fitted, e.g., the rotation–vibration coupling constant, α_e , the anharmonicity constant, $\tilde{\nu}_e x_e$, and, if available, higher spectroscopic constants; and (ii) the occurrence of only small, random-type deviations between the calculated PEC and the corresponding set of RKR points.

The latter criterion has been first tested by Rydberg.⁹ According to which of the criteria for universality is focused on, several strategies of PEC generation and improvement can be made out:

(i) exclusive fit to derivatives $U^{(n)}(R_e)$ at the minimum of the PEC, which is natural for power-series expansions^{14–17} but equally applicable to analytical curves;^{1,6,23}

(ii) additional fit to the potential well depth, $U(\infty) - U(R_e)$, be it D_e ,^{11,12} the ionic limit D_i ,^{20,21,34} or the valence-state dissociation energy D_{vs} ,^{1,3–6}

(iii) additional use of normalization condition set by the quantum mechanical virial theorem;²³

(iv) global fit to all available RKR data,^{9,12,27–33} whereby different analytical functions may have to be spliced together for different domains, e.g., $R < R_e$ and $R \geq R_e$.³³

At first sight, strategy (iv), the PE function generation by global fit, seems to carry the day. However, as noted by Steele et al.,¹² a good global fit with RKR curves does not necessarily result in a satisfactory prediction of α_e and $\tilde{\nu}_e x_e$; for example, the Varshni III function¹¹ “gives good correlation with the RKR curves but is the poorest of all functions in predicting $\tilde{\nu}_e x_e$ ”.¹² Further, Zavitsas’ highly efficient global fit prohibits any assignment of higher derivatives at R_e and spectroscopic constants beyond k_e .³³ Therefore, we shall continue using both criteria for our assessments.

In the following sections, our report¹ on the universality of the VS PEC in the Coulson–Fischer domain up to $R \approx 1.6R_e$ is expanded, and we claim a similar degree of universality for several novel composite PECs over the whole range of distances up to infinity.

3. Methods of Investigation

3.1. Valence-State Potential Energy Function. The VS-PE function describes a hypothetical dissociation process under constraints aiming to maintain the atoms as “they are in the molecule”. According to Ruedenberg, the interference-free parts of the molecular electron density, ρ , and electron-pair density, π , have to be conserved during the dissociation into valence-state atoms.³⁵ As shown in the earlier parts of the series, these requirements are equivalent to keeping the VSEN constant at its equalized molecular value.^{1,3–8} The corresponding VS PEC has the universal form:

$$U_{vs}(R) = -(C/R) + (T/R) \exp(-\lambda R) \quad (1)$$

The parameters C , T , and λ are fitted to R_e , k_e , and $U(\infty) - U(R_e) = D_{vs}$; thence

$$\lambda R_e = k_e R_e^2 / D_{vs} = z; C = D_{vs} (R_e + \lambda^{-1}); T = D_{vs} \lambda^{-1} e^z \quad (2)$$

are obtained.^{4,6} The parameter λ is transferable and obeys the arithmetic mean combining rule.⁶ Note that the transferability is important in reducing the number of species-dependent

molecular parameters. But how can a hypothetical dissociation scheme be of any practical consequence in searching for a universal PEC? The essential argument has been provided more than 50 years ago by Coulson and Fischer,² in fact long before Ruedenberg’s generalized VS concept.³⁵

Coulson and Fischer² clarified the role of electron correlation in bonding. Using the example of H_2 , they determined the best admixture of covalent and ionic states as a function of R by constructing the asymmetric variational wave function:

$$\Psi = [\varphi_A(1) + p(R) \varphi_B(1)][\varphi_B(2) + p(R) \varphi_A(2)] \quad (3)$$

They found two distinct domains for the behavior of the variational parameter $p(R)$:

(i) $p(R) = 1$ up to $R \approx 1.6R_e$, representing the restricted Hartree–Fock (RHF) method with its constant 50% admixture of covalent and ionic states.

(ii) For $R > 1.6R_e$, $p(R)$ falls rapidly to 0 as R increases, and the electrons quickly “go back on to their own atoms”^{2b} as a result of changes in correlation.

The sharp drop in $p(R)$ is known as the Coulson–Fischer transition,^{2b} while the domain (i) may be called the Coulson–Fischer domain. Since the constant $p(R) = 1$ is equivalent to dissociation into MO-theoretical VSAs, we concluded for the spectroscopically most relevant range that the RKR data should be modeled with reference to the VS energies. Therefore, the reference asymptote D_e has been replaced by D_{vs} .^{1,4–6} In accordance with the Coulson–Fischer analysis of the hydrogen molecule, the VS-PE function is a highly effective model of the H_2 ground-state potential energy curve for $R \leq 1.6R_e$. Slater extended the Coulson–Fischer analysis to polar molecules and discussed LiH.³⁶ Harris and Pohl³⁷ discussed the Coulson–Fischer transition for HF, HCl, HBr, and HI. Further support for the argument is drawn from the unrestricted Hartree–Fock (UHF) and the local spin density (LSD) functional models. In dissociating the hydrogen molecule, the local spin density remains strictly zero until a sudden onset of spin polarization at $R \approx 1.6R_e$ for the UHF method³⁸ and $R \approx 2.3R_e$ for the LSD approximation.³⁹ As pointed out by Frost and Musulin, a universal three-parameter PE curve cannot exist with any precision over the whole range of internuclear distances;²⁶ however, much enhancement of scaling and spectroscopic transferability can be gained by a universal reduced curve in the neighborhood of the minimum.^{1,6}

The VS-PE function is reduced to its dimensionless form with $z = k_e R_e^2 / D_{vs}$ as the sole species-dependent parameter^{1,4,6}

$$u_{vs}(s) = 1 - [z + 1 - \exp(-zs)] / z(s + 1) \quad (4)$$

where $s = (R - R_e) / R_e$ is the reduced internuclear displacement. The reduced potential, $u(s) = U(s) / D_{vs}$, has been shifted to $u(0) = 0$.

The original form of the VS-PE function^{1,4} utilizes the molecular parameter set $[R_e, k_e, D_{vs}]$ with

$$D_{vs} = D_e + \sum P^\delta \quad (5)$$

where $\sum P^\delta$ is the VS promotion energy, i.e., the difference between the energy of the partially charged VS atoms and that of the neutral ground-state atoms forming the molecule XY:

$$\sum P^\delta = P_X^0 + P_Y^0 + E_X \quad (6)$$

P_X^0 is the promotion energy of the MO-theoretical VS of the

neutral atom X.^{3,4,8} The partial charge, δ_Y , of atom Y in the single bonded molecule, XY, is calculated according to the VS electronegativity equalization (VS-ENE) as

$$\delta_Y = 2(\chi_X^0 - \chi_Y^0)/(J_X + J_Y) = (\chi_X^0 - \chi_Y^0)/(\eta_X + \eta_Y) \quad (7)$$

where $\chi^0 = \chi_{vs}(1) = (1/2)(I_v + A_v)$ is Mulliken's orbital EN, $J = I_v - A_v$, the one-center two-electron repulsion energy, and $\eta = (1/2)J$, the VS hardness of the active atomic orbital.³⁻⁸ The electronegativity equalization energy

$$E_\chi = -(\chi_X^0 - \chi_Y^0)^2/(J_X + J_Y) = -(1/2)|\delta_Y \Delta \chi^0| \quad (8)$$

stabilizes the system and reduces the VS promotion energy due to partial charge transfer.^{3,4,8} Equations 7 and 8 hold for single bonds. In the general case, including that of double and triple bonds, all the bonding orbitals are coupled in principle; thus the orbital electronegativities mutually influence each other through the chemical hardness matrix (or orbitally resolved hardness tensor), $[\eta_{ij}]$.⁴⁰ In a localized picture, this is equivalent to stating that polarized bonds affect each other's polar character.⁴¹ Several ways to incorporate such coupling have been discussed.^{8,41-45} For localized multiple bonds, the effects of the off-diagonal hardness matrix elements largely cancel each other; thus the coupling of the orbital EN is small.⁴⁵ In this paper, we therefore implement a procedure proposed by Hinze and Bergmann⁴² and treat the double (and triple) bond as a localized four- (and six-) electron bond with averaged EN and hardness parameters. However, the charge dependence of our VSEN scale differs from that of the Hinze-Jaffé scale⁴² and its modification by Bratsch.⁴⁶ For doubly occupied orbitals we arrive at $\chi_{vs}(2) = A_v$, while for unoccupied orbitals we get $\chi_{vs}(0) = I_v$.^{3,4,8} The MgO molecule is an interesting case for demonstrating our ENE method. The valency is 2 (V2) for both atoms, the electron configurations being $(2p_\sigma)^1(2p_\pi)^1(2p,\pi)^2$ on O and a hybridized $(2s\sigma)^1(2p,\pi)^1(2p,\pi)^0$ on Mg. The molecular ground state $^1\Sigma^+$ is described by a rather polar σ,π -double bond and a π -back-donating dative bond of opposite polarity. The (dimensionless) charge number, Q_{Mg} , on the magnesium AIM is calculated as

$$Q_{Mg} = \delta_\sigma + \delta_\pi + (\delta_\pi - 1) = (9.63 - 5.84)10.78^{-1} + (9.63 - 2.37)9.81^{-1} + (9.63 - 2.37 - 9.81)9.81^{-1} = 0.832 \quad (9)$$

In eq 9, our VSEN and VS hardness values are derived from Bratsch's tables.⁴⁶

Allowing for some s-character by isovalent hybridization on O would increase δ_σ ; for a discussion see section 4. The electronegativity equalization energy $E_{\chi,tot}$ is taken as the sum over bond contributions:

$$E_{\chi,tot}/eV = \sum E_{\chi,i}/eV = -(9.63 - 5.84)^2 21.56^{-1} - (9.63 - 2.37)^2 19.62^{-1} - (-2.55)^2 19.62^{-1} = -3.68 \quad (10)$$

The calculation of P^0 and J requires an estimation of the degree of hybridization in the atoms between which the bond resides. An intrinsic hybridization criterion particular to the VSAM method has been developed and led to the operational VS-PE function, labeled as $[R_e, k_e, \alpha_e]$ VS $_\alpha$ PEC,^{1,6} which exclusively uses direct spectroscopic input through the following relations set by the semiempirical curve of eq 4:

$$z_\alpha = 3F = \alpha_e \tilde{v}_e / 2B_e^2 \quad (11)$$

Hence the expression of z in terms of B_e , \tilde{v}_e , and α_e shows

$$z = \frac{k_e R_e^2}{D_{vs}} = \frac{hc \tilde{v}_e^2}{2B_e D_{vs}} = \frac{\alpha_e \tilde{v}_e}{2B_e^2} \quad (12)$$

This allows the introduction of an operational definition for the VS dissociation energy

$$\frac{D_{vs}^{(\alpha)}}{hc} = \frac{B_e \tilde{v}_e}{\alpha_e} \quad (13)$$

Consequently, the spectroscopic constants B_e , \tilde{v}_e , and α_e connected to the first, second, and third derivatives of U at R_e operationally determine the entire three-parameter VS $_\alpha$ PEC of any diatom. This reparametrization is helpful, since some of the dissociation energies for diatoms are not known with the desired degree of accuracy, or the degree of hybridization may be uncertain. The shift from the semiempirical triad $[R_e, k_e, D_{vs}]$ to a fully empirical parameter set $[R_e, k_e, \alpha_e]$ underscores the empirical components of the VS-PE function; nevertheless, the approach remains semiempirical by design due to its reference to theoretical VSAs and their implications for the analytical form of the PEC. The spectroscopic VS dissociation energy, $D_{vs}^{(\alpha)}$, calculated from eq 13, shows good agreement with the theoretical D_{vs} (eq 5). The $D_{vs}^{(\alpha)}/D_{vs}$ ratio averages 1.04 for the VS PECs of 50 diatoms.¹ For these molecules, the three-parameter VS PEC reproduces the RKR data within the Coulson-Fischer domain to an average unsigned error of 1.43% relative to D_e ; the average unsigned error in the repulsive inner limb of the PEC up to R_e amounts to 1.14% of D_e . A discussion of updated and corrected VS PEC parameters and RKR data will be given in section 4. In the following, the VS PEC will remain our potential of choice for the inner limb up to R_e .

3.2. Modeling Coulson-Fischer Type Transitions. For large distances the VS PEC separates from the ground-state RKR curve and asymptotically reaches the VS dissociation limit, i.e., the reference energy (Figure 1) in the single-determinantal description of the molecule.^{3,4} The point has been made that EN and its equalization are meaningful only at the conceptual level where the molecule is described by a single Slater determinant.³ In terms of the Coulson-Fischer analysis, the difference between the VS PEC and the RKR points is a consequence of lacking a variational parameter, such as $p(R)$ of eq 3, so that the Coulson-Fischer transition is not modeled. In accordance with the variation theorem, the VS PEC is found above the energy of the RKR curve in the $R > 1.6R_e$ domain. On the other hand, many three-parameter empirical PECs systematically run below the curve connecting the RKR data of not very polar diatoms; especially the Morse function is known for undercutting the experimental curves.^{11,12} Figures 1 and 2 highlight the relative deviations from RKR, in percent of D_e plotted against the logarithm of the reduced distance, between the Morse and VS curves of H₂ and LiF. The deviations are negative for most of the attractive outer branch of the Morse curve for H₂; thus the homonuclear RKR potential rises more steeply than the empirical PECs. As opposed to semiempirical PE functions,^{1,4,20-23} the variation theorem is of no significance for the assessment of empirical PECs. On the contrary, it is gratifying that the opposite signs of the deviations of the VS PEC and the Morse PEC (Figure 1) provide means for error cancellation in constructing a "composite" PEC that matches the experiment up to $R \rightarrow \infty$ and enforces the asymptotic shift from D_{vs} to D_e .

There is a clear physical picture behind the idea: it is rooted in the bond analyses of Coulson and Fischer^{2,36,37} and Gunnarson

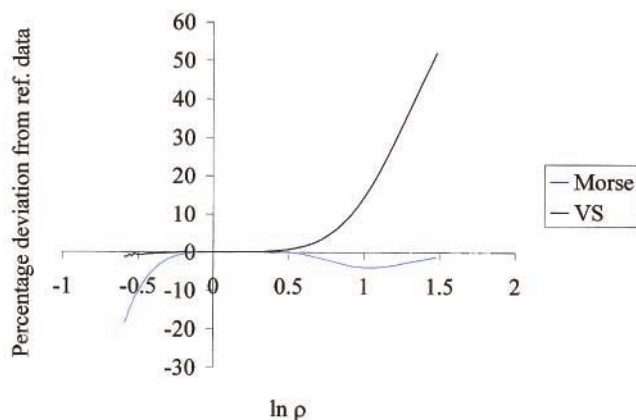


Figure 1. Homonuclear molecules: opposite trends in potential energy difference ($U_{\text{cal}} - U_{\text{ref}}/D_e$) vs $\ln(R/R_e)$. Example: H_2 shown for the Morse (blue) and valence-state VS PEC (black). RKR reference data for H_2 from: Weissman, S.; Vanderslice, J. T.; Battino, R. *J. Chem. Phys.* **1963**, 2226. The ripples at small distances are due to slight RKR inaccuracies.

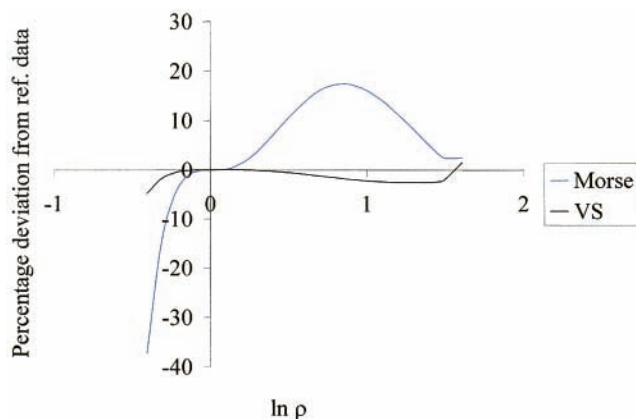


Figure 2. Alkali metal halides: potential energy difference ($U_{\text{cal}} - U_{\text{ref}}/D_e$) vs $\ln(R/R_e)$ shown for LiF; Morse PEC (blue), VS PEC (black). MCSCF ab initio reference data for LiF from ref 47.

and Lundquist.³⁹ Starting with the partially ionic MO-theoretical VS PEC up to R_e , we model the decreasing weight of the “ionic structures” along the dissociation coordinate R by gradually admixing a typical “covalent PEC”, until a dissociation into ground-state atoms is reached. To our knowledge, this is the first approach of its kind. As already pointed out in the original paper, the onset and sharpness of the Coulson–Fischer transition depend on the details of the wave function.^{2a,36,37} If the ansatz is made more flexible, the variation parameter $p(R)$ in eq 3

(i) assumes a value less than unity at the equilibrium internuclear distance $p(R_e) < 1$ and

(ii) slowly decreases in the whole domain $R > R_e$.

Our improved universal PECs reflect this behavior and describe a smooth transition from the VSAM model to the covalent and long-range interaction of ground-state atoms by

(i) a semiempirical account for some post-Hartree–Fock correlation in using $J = I_v - A_v$, instead of the Hartree–Fock repulsion integral J_{HF} , e.g., for hydrogen, $I_v - A_v = 12.844$ eV instead of $J_{\text{HF}}(\text{H}) = 20.42$ eV; and

(ii) gradually phasing in a covalent PEC right from R_e onward.

In other words, we attempt to model a “soft” Coulson–Fischer transition.

3.2.1. Combination of the VS and Morse Potentials. The practical question arises as to which of the three-parameter covalent PECs to combine with the VS PEC. In addition, the

blending ratio as a function of R is crucial. After considerable trial and error—including power series expansions with up to six additional adjustable parameters—we find that the Morse PEC is very adequate for the homonuclear case. The amount of its admixture to the VS PEC is well determined by the normalized Morse function itself. The “soft” transition is achieved at the low cost of the single additional molecular parameter, D_e :

$$0 \leq u_{\text{morse}} = [1 - \exp(-\Delta^{1/2}s)]^2 \leq 1 \quad (14)$$

where $\Delta = k_e R_e^2/2D_e$ is the Sutherland parameter.¹¹ Our first composite PEC, denoted valence-stateMorse (VSM) curve, is

$$\begin{aligned} U_{\text{VSM}} &= U_{\text{vs}} & R < R_e \\ &= U_{\text{vs}}[1 - u_{\text{morse}}] + D_e u_{\text{morse}}^2 & R \geq R_e \end{aligned} \quad (15)$$

The VSM function has four species-dependent parameters R_e , k_e , D_{vs} and D_e , since the Morse and VS potentials share two common parameters, viz., R_e and k_e . A second set of four parameters, $[R_e, k_e, \alpha_e, D_e]$ is provided by the operational definition of the VS PEC in (12) and (13); the resulting PEC will be called the VSM $_{\alpha}$ curve.

3.2.2. Universal Ionic–Covalent Curves (UICC). Toward the other end of the bond polarity scale, for ionic molecules, e.g., LiF, the VS PEC approaches a classic ionic PEC (Hellmann PEC²¹) and properly describes the RKR curve over a larger domain reaching well beyond $R \approx 1.6R_e$. In fact, the ionic domain of very polar PECs extends up to the classical crossing radius $R_x = e^2/4\pi\epsilon_0 J \gg 1.6R_e$. The ionic and covalent structures of the alkali metal halides are prime examples for diabatic states.⁴⁷ The systematic undercutting of the covalent RKR curves by the common empirical curves is changed to the opposite for ionic bonds: after the minimum at R_e , the Morse, Rydberg, and Varshni III PECs rise much too steeply above the RKR values in the outer branch of the curve. This behavior is exemplified in the LiF molecule in Figure 2. A significant modification of (13), viz., a charge-dependent reduction of k_e in the Sutherland parameter, Δ , is needed, to slow the onset of the covalent function at the beginning of the outer branch.⁴⁸ Obviously, several charge-dependent functions are imaginable and could be found by global optimization. In this article, we only test the function

$$f(Q) = \Delta^{1/2}[1 + (1/2)|Q|^{1/2} - |Q|] \quad (16)$$

which smoothly connects $f(0) = \Delta^{1/2}$ and $f(1) = (1/2)\Delta^{1/2}$.

Our charge-dependent modified Morse function $U_{\text{qm}} = D_e u_{\text{qm}}$ normalizes to

$$u_{\text{qm}} = [1 - \exp\{-f(Q)s\}]^2 \quad (17)$$

Combined with the VS PEC we obtain a universal ionic–covalent (UIC) curve:

$$\begin{aligned} U_{\text{UIC}} &= U_{\text{vs}} & R < R_e \\ &= U_{\text{vs}}[1 - u_{\text{qm}}] + D_e u_{\text{qm}}^2 & R \geq R_e \end{aligned} \quad (18)$$

As opposed to direct empirical input from the RKR curve, such as R_e , k_e , or α_e , the charge Q is a different kind of parameter. In our VSENE model, the bond polarity δ and charge Q are obtained from the (secondary^{42b}) atomic properties χ^0 and J according to eqs 7–9. In judging the number and type of the parameters involved in the universal PEC, we have to recall

TABLE 1: Spectroscopic Parameters for Ground-State Diatomic Molecules^a

| molecule | partial charge, Q | $R_e/\text{\AA}$ | $k_e/\text{eV \AA}^{-2}$ | D_e/eV | D_{vs}/eV | B_e/cm^{-1} | $\tilde{\nu}_e/\text{cm}^{-1}$ | $10^3\alpha_e/\text{cm}^{-1}$ | D_{vs}^α/eV |
|-------------------------------|---------------------|------------------|--------------------------|-----------------|--------------------|----------------------|--------------------------------|-------------------------------|---------------------------|
| Homonuclear | | | | | | | | | |
| H ₂ | 0 | 0.7414 | 35.94 | 4.747 | 11.17 | 60.853 | 4401.2 | 3062 | 10.85 |
| Li ₂ | 0 | 2.673 | 1.576 | 1.056 | 3.443 | 0.6726 | 351.43 | 7.040 | 4.163 |
| Na ₂ | 0 | 3.079 | 1.071 | 0.735 | 3.042 | 0.1547 | 159.13 | 0.8736 | 3.494 |
| K ₂ | 0 | 3.924 | 0.613 | 0.552 | 2.472 | 0.05674 | 92.02 | 0.212 | 3.05 |
| Rb ₂ | 0 | 4.2099 | 0.525 | 0.495 | 2.341 | 0.0224 | 57.79 | 0.0558 | 2.876 |
| Cs ₂ | 0 | 4.648 | 0.433 | 0.453 | 2.164 | 0.01174 | 42.09 | 0.023 | 2.64 |
| C ₂ | 0 | 1.243 | 76.0 | 6.32 | 19.0 | 1.8201 | 1855.7 | 18.20 | 23.0 |
| Si ₂ | 0 | 2.246 | 13.47 | 3.242 | 11.33 | 0.2390 | 510.98 | 1.350 | 11.25 |
| N ₂ | 0 | 1.098 | 143.25 | 9.906 | 31.79 | 1.9982 | 2358.6 | 17.81 | 32.81 |
| P ₂ | 0 | 1.894 | 34.75 | 5.08 | 19.72 | 0.3036 | 780.77 | 1.49 | 19.7 |
| O ₂ | 0 | 1.207 | 73.45 | 5.213 | 17.71 | 1.4456 | 1580.2 | 15.93 | 17.78 |
| S ₂ | 0 | 1.889 | 31.16 | 4.414 | 15.15 | 0.2955 | 725.65 | 1.570 | 16.93 |
| ³⁵ Cl ₂ | 0 | 1.988 | 20.13 | 2.514 | 11.35 | 0.2441 | 559.7 | 1.530 | 11.07 |
| ⁷⁹ Br ₂ | 0 | 2.281 | 15.38 | 1.991 | 10.28 | 0.0821 | 325.32 | 0.3206 | 10.33 |
| ¹²⁷ I ₂ | 0 | 2.666 | 10.764 | 1.556 | 8.82 | 0.0374 | 214.5 | 0.114 | 8.75 |
| Same Group Heteronuclear | | | | | | | | | |
| LiNa | -0.034 | 2.889 | 1.306 | 0.881 | 3.220 | 0.3960 | 256.8 | 3.776 | 3.207 |
| SO | 0.242 | 1.493 | 51.78 | 5.44 | 18.76 | 0.7208 | 1149.2 | 5.736 | 18.19 |
| SeO | 0.307 | 1.648 | 41.01 | 4.8 ± 0.2 | 16.6 ± 0.2 | 0.4655 | 914.69 | 3.23 | 16.34 |
| ICl | 0.151 | 2.321 | 14.89 | 2.177 | 10.18 | 0.1142 | 384.29 | 0.536 | 10.16 |
| IBr | 0.098 | 2.469 | 12.91 | 1.834 | 9.56 | 0.0568 | 268.64 | 0.1969 | 9.613 |
| Hydrides | | | | | | | | | |
| LiH | 0.473 | 1.596 | 6.404 | 2.515 | 5.933 | 7.5137 | 1405.65 | 216.65 | 6.044 |
| NaH | 0.498 | 1.887 | 4.878 | 1.98 | 5.26 | 4.9033 | 1171.8 | 137.09 | 5.198 |
| KH | 0.571 | 2.240 | 3.52 | 1.832 | 4.64 | 3.419 | 986.6 | 94.39 | 4.414 |
| RbH | 0.587 | 2.367 | 3.216 | 1.808 | 4.52 | 3.020 | 936.9 | 70.71 | 4.961 |
| CsH | 0.615 | 2.494 | 2.923 | 1.834 | 4.37 | 2.7099 | 891.0 | 66.95 | 4.471 |
| MgH | 0.340 | 1.73 | 7.969 | 1.362 | 6.72 | 5.826 | 1495.2 | 185.8 | 5.813 |
| CaH | 0.450 | 2.003 | 6.11 | 1.78 | 7.26 | 4.277 | 1298.3 | 97.0 | 7.10 |
| CH | -0.08 | 1.124 | 27.95 | 3.65 | 9.51 | 14.448 | 2859.1 | 530.0 | 9.65 |
| SiH | 0.297 | 1.52 | 14.95 | 3.18 | 8.07 ± 0.2 | 7.4996 | 2041.8 | 219.0 | 8.669 |
| NH | 0.006 | 1.037 | 37.25 | 3.63 | 10.49 | 16.699 | 3282.3 | 649.0 | 10.47 |
| OH | -0.298 | 0.9706 | 48.98 | 4.624 | 12.82 | 18.871 | 3735.2 | 714.0 | 12.23 |
| SH | -0.130 | 1.345 | 26.59 | 3.547 | 10.52 | 9.5995 | 2711.6 | 278.5 | 11.59 |
| HF ^b | 0.415 | 0.9168 | 60.24 | 6.114 | 13.53 | 20.956 | 4138.32 | 795.8 | 13.51 |
| HCl ^b | 0.320 | 1.275 | 32.32 | 4.617 | 12.352 | 10.593 | 2990.95 | 307.2 | 12.79 |
| AgH | 0.287 | 1.618 | 11.38 | 2.4 ± 0.1 | 6.78 ± 0.1 | 6.50 | 1759.7 | 202.1 | 6.962 |
| CuH | 0.280 | 1.463 | 13.74 | 2.85 | 7.31 | 7.9441 | 1941.26 | 256.3 | 7.44 |
| Oxides and Sulfides | | | | | | | | | |
| BeO | 0.55 | 1.331 | 46.94 | 4.6 ± 0.1 | 15.0 ± 0.1 | 1.651 | 1487.32 | 19.0 | 16.0 |
| MgO | 0.83 | 1.749 | 21.77 | 2.56 | 11.96 | 0.5743 | 785.0 | 5.0 | 11.2 ± 0.2 |
| NO | -0.052 | 1.151 | 99.85 | 6.614 | 22.78 | 1.7042 | 1904.2 | 17.7 | 22.67 |
| CS | 0.414 | 1.535 | 53.12 | 7.435 | 20.17 | 0.820 | 1285.15 | 5.920 | 22.06 |
| SiS | 0.38 | 1.929 | 30.91 | 6.466 | 19.34 | 0.3035 | 749.64 | 1.47 | 19.23 |
| PbS | 0.337 | 2.287 | 18.77 | 3.52 | 13.16 | 0.1163 | 429.17 | 0.435 | 14.23 |
| Metal Halides | | | | | | | | | |
| LiF | 0.822 | 1.564 | 15.48 | 6.00 | 7.82 | 1.345 | 910.57 | 20.29 | 7.84 |
| NaF | 0.844 | 1.926 | 10.99 | 4.98 | 6.57 | 0.4369 | 535.66 | 4.559 | 6.368 |
| BeF | 0.625 | 1.361 | 35.06 | 6.24 | 12.66 | 1.4889 | 1247.36 | 17.60 | 13.08 |
| MgF | 0.708 | 1.750 | 19.49 | 4.67 | 10.26 | 0.5192 | 711.69 | 4.480 | 10.23 |
| AlF | 0.785 | 1.654 | 26.58 | 6.94 | 9.23 | 0.5525 | 802.3 | 4.984 | 11.02 |
| GaF | 0.800 | 1.774 | 21.26 | 6.02 | 8.31 | 0.360 | 622.2 | 2.864 | 9.700 |
| NaCl | 0.814 | 2.361 | 6.788 | 4.29 | 5.71 | 0.2181 | 366.0 | 1.625 | 6.076 |

^a Conversion factors: $\text{eV \AA}^{-2} = 16.02 \text{ N m}^{-1}$, $\text{eV}/hc = 8065.5 \text{ cm}^{-1}$. ^b 5% and 14.4% s-character was used for F and Cl in the calculation of VS for HF and HCl, respectively.

the fact that results derived from the study of atoms are traditionally treated as free information for molecular studies.^{42,49,50} As mentioned above (section 3.1), the transferability property of λ potentially allows reducing the number of species-dependent parameters by using $\lambda_{XY} = (1/2)(\lambda_{XX} + \lambda_{YY})$.⁶

We further define the closely related five-parameter PE function UIC_α with the parameter set $[R_e, k_e, \alpha_e, D_e, Q]$. In analogy to the above VSM_α PEC, the UIC_α function is based on the operational definition of $D_{vs}^{(\alpha)}$ in (13). An obvious effect of this adjustment to the experimental parameter α_e is that the third derivative $U'''(R_e)$ matches that of the reference RKR or ab initio PEC. As mentioned in section 2, this is a standard procedure

for improving PECs.^{28c} While u_{qm} (17) is unaffected, the only change in (18) is the replacement of U_{vs} by the VS_α PEC of ref 1.

4. Results and Discussion

Equations 15 and 18 with the input parameters listed in Table 1 allow one to construct the UIC and UIC_α curves for 50 molecules. The input data compiled in ref 1 have been revised and updated. As exemplified in section 3.1, the charge Q has been reevaluated for all oxides and sulfides. This in turn affects D_{vs} as calculated from eqs 6–10 and is shown in Table 1. Note that $Q = 0$ is trivial for homonuclear diatoms, and thus the

UIC curves are identical to the respective four-parameter VSM PECs. New, more accurate, or extended experimental data have been incorporated for the Rb₂,⁵¹ Br₂,⁵² ICl,⁵³ and NaH⁵⁴ ground-state PECs. As proposed by Bratsch,⁴⁶ halogen σ -orbitals are considered to have a hybridization of 14.4% s-character, exceptions being fluorine (5% s-character in HF^{1,4,6}) and the alkali metal halides (pure p AOs^{1,4,6}).

Multiple bonds need a special discussion. The increase in bond order from single, through double, to triple bonds has a bearing on the amount of hybridization of σ -bonded orbitals. The π -bond compresses the molecules N₂, P₂, and O₂ below the optimal σ -bond length into the repulsive σ -domain, where hybridization does not pay off in the overall energy balance.⁴ In addition, shorter bonds greatly enhance the interpenetration of the interference-free charge densities of the VS atoms, and lower the quasiclassical energy, E_{QC} .^{4,55} For multiple bonds a large part of the hybridization energy is regained by such promotion-induced “quasiclassical stabilization”.⁵⁵ For, e.g., N₂, D_{vs} changes only by 3% when the s-character of the σ -bond is increased from 0 to 50%.^{4,55} We therefore obtain good results by neglecting $E_{hy} - E_{QC}$ altogether, as if there were no hybridization. This conclusion is also supported by the analysis of hybridization in localized MOs.⁵⁶ We now revisit the O₂ case, as new insights have emerged. According to Bratsch, oxygen group atoms should have about (100/6)% \approx 16.7% s-character in their single bonds.⁴⁶ However, O₂ is similar to N₂, insofar as (i) the isovalent hybridization is reduced because the σ -bond is pushed into its repulsive domain by a bond shortening of $\Delta R_e/R_e \approx 10\%$ and (ii) the remaining hybridization energy is largely canceled by quasiclassical stabilization. In calculating the VS bond energy D_{vs} , we start a constrained dissociation of the O₂ molecule and keep the on-site pair repulsion energy frozen until reaching the valency 2 (V2) configuration. Per oxygen AIM, we keep $n(\sigma^{\uparrow})n(\sigma^{\downarrow})J_{\sigma} = (1/2)^2J_{\sigma}$ and $[2(3/4)^2 - 1]J_{p\pi} = (1/8)J_{p\pi}$ promotion energy increments which are additional to the ground-state pair repulsion energy. As with the nitrogen molecule, we assume the σ -bond to be of pure p-character and thus $J_{\sigma} = J_{p\pi}$. As the average V2 configuration energy is 0.50 eV above the ³P₂ ground state,⁴⁶ the total VS promotion energy and D_{vs} of O₂ are therefore

$$\sum P(O) = 2[0.50 + (3/8)15.33] \text{ eV} = 12.50 \text{ eV} \quad (19)$$

and

$$D_{vs}(O_2) = D_e(O_2) + \sum P(O) = 5.213 \text{ eV} + 12.50 \text{ eV} = 17.71 \text{ eV} \quad (20)$$

This result is in excellent agreement with the operational

$$D_{vs}^{(\alpha)}(O_2) = hcB_e \tilde{\nu}_e / \alpha_e = 17.78 \text{ eV} \quad (21)$$

We revise the view held earlier, that oxygen was an exceptional molecule, for which the interference-free part of the molecular energy cannot be retrieved by our standard promotion process.^{1,4} On the other hand, $R_e(S_2)$ is not too different from the standard single bond length⁵⁷ and the change in E_{QC} does not simulate the absence of hybridization; we, therefore, use Bratsch’s hybridization rule (16.7% s-character) for sulfur and selenium compounds.

Because of their relatively low RKR range, we consider the RKR and some D_e data for AgCl, AlF, C₂, GaCl, GaF, Si₂, SiH, and SiS (all discussed in ref 1) incomplete and inconclusive for our extended purpose. These molecules have not been compared with RKR and/or ab initio data (Table 3) as we study

TABLE 2: Average Unsigned Errors in the Spectroscopic Constant, F , Calculated by the VS and UIC PECs^a

| molecule | Sutherland param, Δ | VS param, z | F | F_{obs} | % unsigned error, δF |
|--------------------------|----------------------------|-----------------|-----------------|---------------|------------------------------|
| Homonuclear | | | | | |
| H ₂ | 2.080 | 1.769 | 0.590 | 0.606 | 2.64 |
| Li ₂ | 5.332 | 3.27 | 1.090 | 0.911 | 19.6 |
| Na ₂ | 6.907 | 3.338 | 1.113 | 0.968 | 14.9 |
| K ₂ | 8.550 | 3.818 | 1.273 | 1.030 | 23.6 |
| Rb ₂ | 9.402 | 3.975 | 1.325 | 1.080 | 22.7 |
| Cs ₂ | 10.349 | 4.323 | 1.441 | 1.18 | 22.1 |
| C ₂ | 9.290 | 6.18 | 2.06 | 1.70 | 21.2 |
| Si ₂ | 10.480 | 5.997 | 1.999 | 2.013 | 0.70 |
| N ₂ | 8.717 | 5.433 | 1.811 | 1.755 | 3.19 |
| P ₂ | 12.27 | 6.321 | 2.107 | 2.11 | 0.14 |
| O ₂ | 10.263 | 6.042 | 2.014 | 2.008 | 0.30 |
| S ₂ | 11.762 | 6.854 | 2.285 | 2.19 | 4.34 |
| Cl ₂ | 15.82 | 7.02 | 2.34 | 2.40 | 2.5 |
| Br ₂ | 20.12 | 7.793 | 2.60 | 2.58 | 0.78 |
| I ₂ | 24.584 | 8.674 | 2.891 | 2.914 | 0.79 |
| Same Group Heteronuclear | | | | | |
| LiNa | 6.204 | 3.385 | 1.128 | 1.031 | 9.41 |
| SO | 10.63 | 6.152 | 2.051 | 2.11 | 2.80 |
| SeO | 12.13 | 6.710 | 2.237 | 2.272 | 1.54 |
| ICl | 18.42 | 7.880 | 2.627 | 2.632 | 0.19 |
| IBr | 21.456 | 8.232 | 2.744 | 2.729 | 0.55 |
| Hydrides | | | | | |
| LiH | 3.243 | 2.749 | 0.916 | 0.900 | 1.78 |
| NaH | 4.386 | 3.302 | 1.101 | 1.114 | 1.17 |
| KH | 4.826 | 3.806 | 1.270 | 1.334 | 4.80 |
| RbH | 4.983 | 3.986 | 1.329 | 1.211 | 9.74 |
| CsH | 4.957 | 4.161 | 1.387 | 1.356 | 2.29 |
| MgH | 8.757 | 3.549 | 1.183 | 1.368 | 13.5 |
| CaH | 6.885 | 3.317 | 1.106 | 1.151 | 3.91 |
| CH | 4.837 | 3.713 | 1.238 | 1.220 | 1.48 |
| SiH | 5.422 | 4.28 | 1.427 | 1.328 | 7.45 |
| NH | 5.518 | 3.819 | 1.273 | 1.275 | 0.16 |
| OH | 4.938 | 3.559 | 1.20 | 1.247 | 3.77 |
| SH | 6.630 | 4.471 | 1.490 | 1.383 | 7.74 |
| HF | 4.137 | 3.74 | 1.247 | 1.250 | 0.24 |
| HCl | 5.690 | 4.254 | 1.418 | 1.369 | 3.58 |
| AgH | 6.233 | 4.394 | 1.465 | 1.426 | 2.73 |
| CuH | 5.160 | 4.023 | 1.341 | 1.314 | 2.06 |
| Oxides and Sulfides | | | | | |
| BeO | 9.0 | 5.54 \pm 0.05 | 1.85 \pm 0.02 | 1.73 | 6.9 \pm 1.1 |
| MgO | 13.0 | 5.57 | 1.86 | 2.0 \pm 0.1 | 7.0 \pm 5.0 |
| NO | 10.00 | 5.807 | 1.936 | 1.945 | 0.46 |
| CS | 8.417 | 6.205 | 2.068 | 1.891 | 9.36 |
| SiS | 8.894 | 5.947 | 1.982 | 1.994 | 0.60 |
| PbS | 13.957 | 7.460 | 2.487 | 2.30 | 8.13 |
| Metal Halides | | | | | |
| LiF | 3.155 | 4.842 | 1.614 | 1.61 | 0.25 |
| NaF | 4.09 | 6.205 | 2.068 | 2.132 | 3.00 |
| BeF | 5.204 | 5.130 | 1.710 | 1.651 | 3.57 |
| MgF | 6.39 | 5.818 | 1.939 | 1.926 | 0.69 |
| AlF | 5.207 | 7.878 | 2.626 | 2.20 | 19.3 |
| GaF | 5.556 | 8.003 | 2.668 | 2.292 | 16.4 |
| NaCl | 4.410 | 6.627 | 2.209 | 2.084 | 6.0 |
| GaCl | 5.583 | 7.847 | 2.616 | 2.151 | 21.6 |
| overall average | | | | | 6.37 |

^a The third derivative and hence the F value of both curves are identical.

PECs up to the dissociation limit. We take this opportunity to correct a mixup that occurred in ref 1: Table 1 referred to the ³ Π_u state of C₂, but Table 2 used the ground-state value for α_e . Further, the ground-state force constant for S₂ has to be corrected to $k_e = 31.16 \text{ eV } \text{Å}^{-2}$. The PECs of CuH, Al₂, and F₂ remain

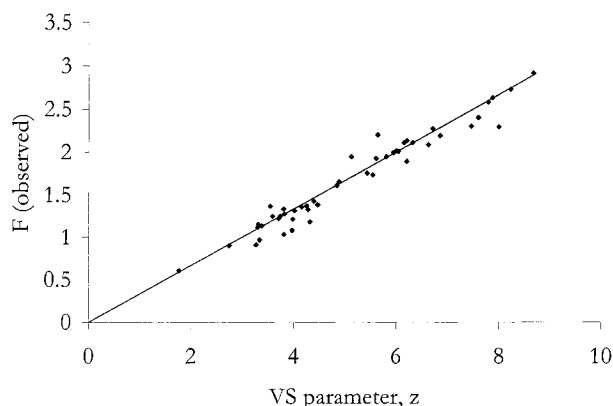


Figure 3. Observed rotation–vibration coupling constant F_{obs} vs calculated valence-state parameter $z = k_e R_e^2 / D_{\text{vs}}$ for 50 molecules of Table 2. The line shows the valence state potential prediction: $F_{\text{vs}}(z) = z/3$.

excluded for reasons discussed in our preceding paper.¹ Additionally, a “hump” in the PEC of CuH has been reported,³³ so that more experimental data are needed for this molecule. In general, the available RKR data for the coinage metal hydrides do not allow the determination of precise D_e values; cf. the error margin indicated for AgH.⁵⁸ The molecules tested by us are those for which we have sufficient RKR and/or reliable spectroscopic data available.

4.1. Calculation of the Rotation–Vibration Coupling Constant F . The PE function is considered as having universal character if the observed spectroscopic constants $F_{\text{obs}} = \alpha_e \tilde{\nu}_e / 6B_e^2$ and $G_{\text{obs}} = 8\tilde{\nu}_e x_e / B_e$ are well represented by the calculated F and G obtained from simple relations involving the appropriate dimensionless molecular parameter.^{4,11,12} We now check this criterion for the UIC, Morse, Rydberg, and Varshni III PECs. The $F_{\text{UIC}\alpha}$ function is not included in the comparison, as it has been operationally defined to fulfill $F_{\text{UIC}\alpha} = F_{\text{obs}}$ and $z_\alpha = 3F_{\text{obs}}$. Note that Zavitsas’ universal PEC does not allow any assignment of F , or α_e , because its third and higher derivatives are undefined at R_e ; this, however, does not detract from its universal character. Our UICs show a similar derivative discontinuity at R_e from the fourth derivative onward.

For the UIC function, the first and second derivatives at the minimum fit the necessary requirements $U'(R_e) = 0$ and $U''(R_e) = k_e = zD_{\text{vs}}/R_e^2$, and the ratio $-U'''(R_e)R_e/U''(R_e) = -l_e R_e / k_e = 3 + z$ is identical with the corresponding ratio of the VS PEC. This ratio, in turn, determines $F_{\text{UIC}}(z) = -1 - l_e R_e / 3k_e = z/3$. For our 50 molecules, with $0 \leq Q < 0.9$, the plot of F_{obs} vs z gives the regression line $F_{\text{obs}} = 0.0303 + 0.326z$, and the correlation coefficient $r = 0.989$ (Figure 3). The slope 0.326 is almost identical with that reported for a different set of 23 molecules,⁴ and the intercept is practically zero; thus, the theoretical curve $F_{\text{UIC}}(z) = z/3$ is closely matched. The comparison of the calculated F_{UIC} with experimental values⁵⁹ for our set of molecules shows an average unsigned error of 6.37%. No separation into ionic and covalent compounds is detectable in Figure 3.

Since $z = k_e R_e^2 / D_{\text{vs}}$, the dimensionless vibration–rotation coupling constant F_{UIC} is defined by these three parameters even for our five-parameter UIC functions. The following comparison with the F values of three-parameter empirical PECs is therefore entirely unbiased. For the Morse,²⁴ Rydberg,⁹ and Varshni functions,¹¹ the appropriate dimensionless parameter is the Sutherland parameter, $\Delta = k_e R_e^2 / 2D_e$. For these PECs the following functional relations hold between F and Δ :¹¹

$$F_{\text{morse}} = \Delta^{1/2} - 1 \quad F_{\text{rydberg}} = (2/3)(2\Delta)^{1/2} - 1 \\ F_{\text{varshni}} = \Delta^{1/2} + 2\Delta^{-1/2} - 2 \quad (22)$$

Figure 4 plots the experimental F_{obs} versus $\Delta^{1/2}$ and shows the variance of the calculated F_{morse} , F_{rydberg} , and F_{varshni} curves from the experimental data. The straight line (22) obtained for the Morse PEC appears to divide the ionic molecules centered above in the top left from the more covalent species situated mostly below and to the right of the Morse line. The Rydberg and Varshni III PECs slightly improve the correlation with covalent and less polar bonds; on the other hand, they are even less suited for the highly ionic diatoms. These graphical plots of F vs $\Delta^{1/2}$ reveal a “spectroscopic gap”:³⁴ a separation between the positions of ionic and covalent molecules with each class following a different trend. For the whole set, the best regression line for F_{obs} vs $\Delta^{1/2}$ through the Morse and Rydberg intercept at $F(0) = -1$ has the slope 0.902, which is significantly below the “theoretical” value of 1 for the Morse and nearer that of 0.9248 for the Rydberg function; see (22). However, the correlation coefficient $r = 0.283$ is very low. The comparison of Figures 3 and 4 visibly documents the superior performance of the UIC (and VS PE) function(s) in calculating the rotation–vibration coupling constant, i.e., essentially the third derivative of the RKR curve at R_e .

For our 50 molecules, the average unsigned errors of the Morse, Rydberg, and Varshni III PECs amount to 32%, 30%, and 26% of F , respectively. Thus, in calculating the third derivative, $U'''(R_e)$, the UIC and VS PE functions are almost an order of magnitude more accurate than the Morse, Rydberg, and Varshni III PECs. Hydrogen is again particularly well represented with -3% deviation, compared to -28% for the Morse, -41% for the Rydberg, and $+39.8\%$ for the Varshni III functions. The values of individual errors in $F_{\text{UIC}} = F_{\text{vs}}$ for the molecules tested correspond to those of the dissociation energy ratios, $D_{\text{vs}}^{(\alpha)} / D_{\text{vs}}$; cf. section 3.1 in ref 1.

4.2. Deviation of the UIC Curves from RKR and ab Initio Data. Table 3 lists the average unsigned errors, $\delta U / D_e$, obtained by the UIC, $F_{\text{UIC}\alpha}$, Morse, Rydberg, and Varshni III PECs for individual molecules and the overall average of a set of 42:

$$\frac{\delta U}{D_e} = \frac{\sum_i^{\text{ref}} |U_{\text{cal}}(R_i) - U_{\text{ref}}(R_i)|}{nD_e} \times 100\% \quad (23)$$

where $U_{\text{cal}}(R_i)$ is the calculated potential energy at a given RKR or ab initio reference point, R_i , and n is the total number of points reported.

We first discuss the detailed results for some representative bonds, viz., two homonuclear molecules H_2 (Figure 5) and Li_2 (Figure 6), the ionic LiF (Figure 7), and two hydrogen-containing diatoms of opposite polarity, LiH (Figure 8) and OH (Figure 9). These figures show the signed relative deviations $[U_{\text{cal}}(R_i) - U_{\text{ref}}(R_i)] / D_e$ as a function of the reduced distance R/R_e . For H_2 , our UICs, i.e., the four-parameter VSM and $F_{\text{UIC}\alpha}$ PECs (15) represent highly significant improvements. The repulsive inner limb is almost perfectly modeled (cf. ref 1), and the deviations in the remaining spectroscopically important domain, up to $R < 3R_e$, are an order of magnitude smaller than those of the empirical PECs (Figure 5). The small ripples around $R \approx 0.5R_e$ result from slight inaccuracies of the experimental RKR data. On average over the whole range of distances covered by the RKR data for H_2 , the performance of

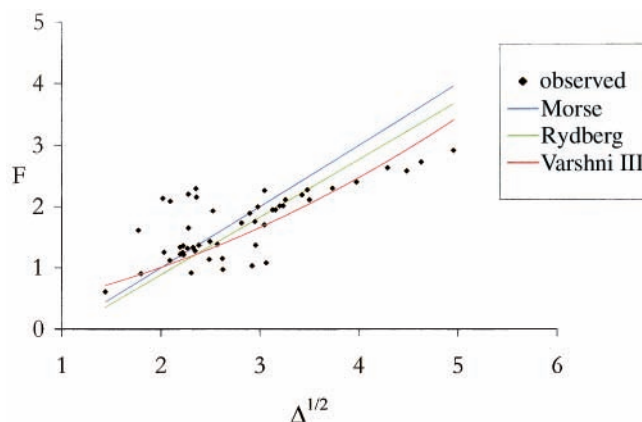


Figure 4. F_{obs} vs square root of Sutherland parameter $\Delta^{1/2}$ for 50 molecules of Table 2. The Morse, Rydberg, and Varshni III predictions are drawn.

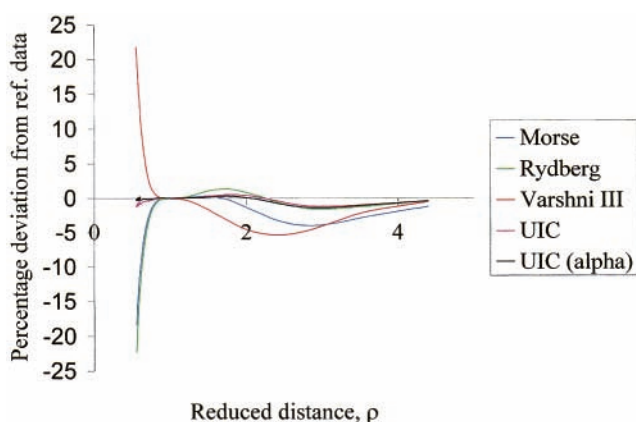


Figure 5. Hydrogen molecule: relative potential energy difference $(U_{\text{cal}} - U_{\text{ref}})/D_e$ over reduced distance, R/R_e , shown for the UIC $_{\alpha}$ (black), UIC (pink), Varshni III (red), Rydberg (green), and Morse (blue) PECs. Reference as in Figure 1.

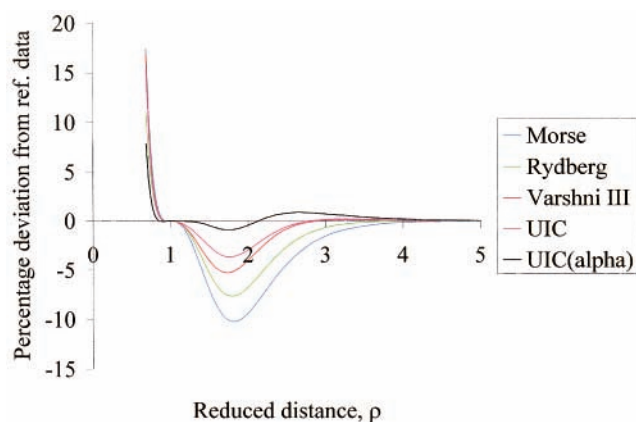


Figure 6. Lithium molecule: relative potential energy difference $(U_{\text{cal}} - U_{\text{ref}})/D_e$ over reduced distance, R/R_e , shown for the UIC $_{\alpha}$ (black), UIC (pink), Varshni III (red), Rydberg (green), and Morse (blue) PECs. RKR + IPA reference data from: Hessel, M. M.; Vidal, C. R. *J. Chem Phys.* **1979**, *70*, 4439.

the UICCs is exceeds that of three-parameter PECs by more than an order of magnitude (Table 3).

Figure 6 highlights a systematic trend typical for the weak bonds in the alkali metal diatoms. All of the empirical PECs are far too steep in the inner limb, but too shallow between $1 < R/R_e < 3$, where the maximal deviation is around -10% of D_e at $R \approx 2R_e$. As reported earlier,^{4,5} the rotation–vibration

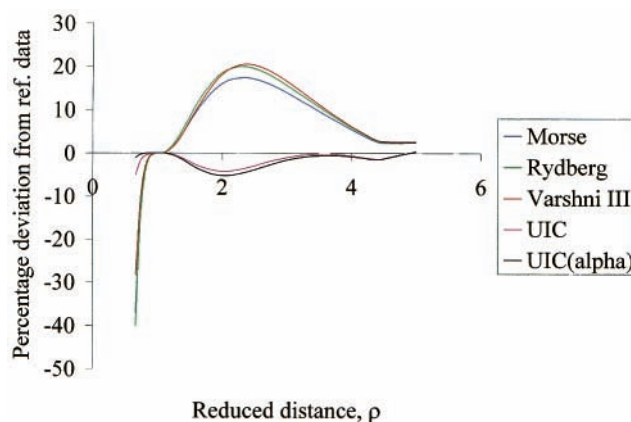


Figure 7. Lithium fluoride (partial charge $Q_{\text{Li}} = 0.822$): relative potential energy difference $(U_{\text{cal}} - U_{\text{ref}})/D_e$ over reduced distance, R/R_e , shown for the UIC $_{\alpha}$ (black), UIC (pink), Varshni III (red), Rydberg (green), and Morse (blue) PECs. Reference as in Figure 2.

coupling is poorly represented by both the VS PE and empirical functions. The operational fit to α_e in our VSM $_{\alpha}$ function reduces the average unsigned errors, $\delta U/D_e$, of the alkali metal diatoms by up to a factor of 2 (Table 3). However, a fifth molecular parameter, i.e., a further empirical fit to $\tilde{v}_e x_e$ or to both the third and fourth derivatives at R_e , is needed, to obtain results of similar accuracy as for H_2 with just four parameters. This has been done using the extended Rydberg function.¹³ Good-quality results have been obtained with Zavitsas' globally fitted six-parameter PEC.³³ We have argued that the different shapes of the RKR curves for hydrogen and the alkali metal diatoms are connected to the different types of valence-electron correlation in the molecules.⁴ The valence correlation is mainly of the angular (or “in–out”) type for the alkali metal diatoms, but of the “left–right” character for H_2 . The fact that the Hartree–Fock approximation barely reproduces 17% of the bond dissociation energy of Li_2 ⁶¹ appears to be important, since our covalent VS reference energy is rooted in the restricted HF model. Incidentally, a similar connection may be operative in the case of the fluorine molecule, where both the Hartree–Fock and VS PEC perform badly.⁴

High level ab initio reference data are available for the PECs of LiF ,⁴⁷ NaF ,⁶² and NaCl .⁶³ As mentioned in section 3.1 and shown in Figure 7, large positive deviations of up to $+20\%$ of D_e characterize the Morse and other empirical PECs of the alkali metal halides. Note the opposite shapes of the deviations in the Figures 6 and 7. Our five-parameter UICCs evenly reduce the errors for LiF (Figure 7) and NaF by an order of magnitude to a maximum positive deviation of 2%, and an average unsigned error of about 1%. The latter error is about 2% for the NaCl molecule, as opposed to 7–8% with the three-parameter curves (Table 3). Further improvement of our results is predictable by fixing the fifth parameter to reproduce the anharmonicity constant.

The 14 hydrogen-containing diatoms in Table 1 form an interesting group with a variety of ground-state electronic configurations and different, sometimes opposite bond polarities, δ . The UIC curves for most of these have been compared with the reliable ab initio data of Meyer and Rosmus.⁶⁴

Figure 8 plots the results for LiH in the region $0.6 < R/R_e < 3.2$. None of the functions tested does particularly well, but the Varshni III curve reproduces the RKR data better than either the UIC or UIC $_{\alpha}$ PECs. Except for KH , the alkali metal hydrides are generally better represented through the Varshni III than the UIC functions (Table 3). Out of the set of 42 molecules,

TABLE 3: Average Unsigned Errors, $\delta U/D_e$, for UIC and UIC $_{\alpha}$ PECs: Morse, Rydberg, and Varshni III PECs Included for Comparison

| molecules | UIC % $\delta U/D_e$ | UIC $_{\alpha}$ % $\delta U/D_e$ | Morse % $\delta U/D_e$ | Rydberg % $\delta U/D_e$ | Varshni III % $\delta U/D_e$ | U_{\max}/D_e | ref ^a |
|--------------------------|----------------------|----------------------------------|------------------------|--------------------------|------------------------------|----------------|------------------|
| Homonuclear | | | | | | | |
| H ₂ | 0.57 | 0.35 | 5.66 | 6.32 | 7.09 | 0.933 | a |
| Li ₂ | 2.10 | 0.71 | 4.71 | 2.87 | 2.97 | 0.69 | b |
| Na ₂ | 4.17 | 2.47 | 11.63 | 8.90 | 7.96 | 0.99 | c |
| K ₂ | 3.60 | 2.62 | 9.93 | 7.94 | 6.42 | 0.83 | d |
| Rb ₂ | 3.60 | 2.00 | 10.8 | 8.71 | 6.91 | 0.99 | 51 |
| Cs ₂ | 2.57 | 1.87 | 6.96 | 5.73 | 4.33 | 0.678 | e |
| N ₂ | 0.76 | 0.47 | 1.58 | 0.64 | 0.30 | 0.551 | f |
| P ₂ | 1.06 | 0.96 | 2.70 | 1.82 | 0.84 | 0.514 | f |
| O ₂ | 0.76 | 0.73 | 2.09 | 1.48 | 1.38 | 0.707 | g |
| S ₂ | 1.27 | 1.32 | 1.84 | 1.91 | 1.86 | 0.547 | h |
| Cl ₂ | 0.86 | 1.79 | 6.62 | 4.14 | 1.46 | 1.0 | i |
| Br ₂ | 0.23 | 0.27 | 3.34 | 2.42 | 1.38 | 0.64 | 52 |
| I ₂ | 2.06 | 2.19 | 8.84 | 5.86 | 2.90 | 1.0 | j |
| Same Group Heteronuclear | | | | | | | |
| LiNa | 1.54 | 1.25 | 6.33 | 4.17 | 3.52 | 0.961 | k |
| SO | 0.54 | 0.56 | 1.05 | 1.07 | 1.04 | 0.463 | l |
| SeO | 0.15 | 0.11 | 0.21 | 0.17 | 0.31 | 0.224 | f |
| ICl | 0.62 | 0.64 | 5.60 | 3.31 | 1.30 | 0.997 | 53 |
| IBr | 0.30 | 0.31 | 2.46 | 2.31 | 2.23 | 0.332 | m |
| Hydrides | | | | | | | |
| LiH | 2.71 | 2.48 | 3.60 | 3.85 | 1.76 | 0.975 | n |
| NaH | 2.78 | 2.78 | 2.68 | 3.00 | 1.14 | 0.973 | 54 |
| KH | 0.84 | 0.99 | 2.42 | 1.79 | 2.32 | 0.998 | o |
| RbH | 1.85 | 1.26 | 0.69 | 0.84 | 0.49 | 0.574 | p |
| CsH | 6.49 | 3.56 | 2.90 | 2.09 | 1.36 | 0.994 | p |
| MgH | 1.21 | 1.43 | 11.45 | 11.67 | 11.01 | 0.967 | 64 |
| CaH | 1.16 | 1.29 | 4.03 | 2.95 | 2.41 | 0.603 | q |
| CH | 1.41 | 1.38 | 0.76 | 0.81 | 1.23 | 0.961 | 64 |
| NH | 0.73 | 0.74 | 1.17 | 0.55 | 0.94 | 0.74 | 64 |
| OH | 0.55 | 0.63 | 1.85 | 1.97 | 1.00 | 0.753 | 64 |
| SH | 0.36 | 0.26 | 0.72 | 0.26 | 0.10 | 0.415 | 64 |
| HF | 1.46 | 1.43 | 4.46 | 5.37 | 3.14 | 0.979 | r |
| HCl | 1.57 | 1.26 | 2.98 | 2.81 | 1.38 | 0.989 | s |
| AgH | 1.02 | 0.63 | 1.48 | 1.38 | 0.81 | 0.76 | f |
| Oxides and Sulfides | | | | | | | |
| BeO | 0.69 | 0.36 | 0.32 | 0.17 | 0.51 | 0.340 | f |
| MgO | 1.28 | 1.52 | 1.57 | 1.58 | 1.52 | 0.280 | f |
| NO | 0.77 | 0.80 | 2.29 | 1.03 | 0.52 | 1.0 | f |
| CS | 0.55 | 0.17 | 0.11 | 0.27 | 0.59 | 0.288 | t |
| PbS | 0.49 | 0.41 | 0.72 | 0.45 | 0.13 | 0.237 | f |
| Metal Halides | | | | | | | |
| LiF | 1.01 | 0.82 | 7.59 | 8.44 | 8.32 | 0.973 | 47 |
| NaF | 1.20 | 1.21 | 10.03 | 10.94 | 10.80 | 0.907 | 62 |
| BeF | 0.77 | 0.69 | 1.10 | 1.61 | 1.71 | 0.385 | f |
| MgF | 0.25 | 0.20 | 0.42 | 0.53 | 0.59 | 0.239 | f |
| NaCl | 2.16 | 1.84 | 6.68 | 7.63 | 8.09 | 0.931 | 63 |
| overall average | 1.42 | 1.16 | 3.92 | 3.38 | 2.76 | | |

^a RKR and ab initio data were obtained from the references highlighted in text as well as the following: (a) Weissman, S.; Vanderslice, J. T.; Battino, R. *J. Chem. Phys.* **1963**, *37*, 2226. (b) (i) Kusch, P.; Hessel, M. M. *J. Chem. Phys.* **1977**, *67*, 586. (ii) Hessel, M. M.; Vidal, C. R. *J. Chem. Phys.* **1979**, *70*, 4439. (c) (i) Kusch, P.; Hessel, M. M. *J. Chem. Phys.* **1978**, *68*, 2591. (ii) Kato, H.; Matsui, T.; Noda, C. *J. Chem. Phys.* **1982**, *76*, 5678. (d) Ross, A.; Crozet, P.; d'Incan, J.; Effantin, C. *J. Phys. B* **1986**, *19*, L145. (e) Vidal, C. R.; Raab, M.; Hönig, G.; Demtröder, W. *J. Chem. Phys.* **1982**, *76*, 4370. (f) Jenč, F. Private communication. (g) Saxon, R. P.; Liu, B. *J. Chem. Phys.* **1977**, *67*, 5432. (h) Saxon, R. P.; Liu, B. *J. Chem. Phys.* **1980**, *73*, 5174. (i) Douglas, A. E.; Hoy, A. R. *Can. J. Phys.* **1975**, *53*, 1965. (j) Tellinghuisen, J. *J. Mol. Spectrosc.* **1980**, *82*, 225. (k) Schmidt-Mink, I.; Müller, W.; Meyer, W. *Chem. Phys. Lett.* **1984**, *112*, 120. (l) Verma, K. K.; Reddy, F. *J. Mol. Spectrosc.* **1977**, *67*, 360. (m) Coxon, J. A. *J. Mol. Spectrosc.* **1980**, *82*, 264. (n) Vidal, C. R.; Stwalley, W. *J. Chem. Phys.* **1982**, *77*, 883. (o) Hussein, K. *Chem. Phys. Lett.* **1986**, *124*, 105. (p) Stwalley, W. C.; Zemke, W. T.; Yang, S. C. *J. Phys. Chem. Ref. Data* **1991**, *20*, 153. (q) Rao, T. R.; Reddy, F.; Rao, A. *J. Mol. Struct. (THEOCHEM)* **1983**, *105*, 249. (r) Bredford, E. J.; Engelke, F. *Chem. Phys. Lett.* **1980**, *75*, 132. (s) Coxon, J. A.; Ogilvie, J. F. *J. Chem. Soc., Faraday Trans. 2* **1982**, *78*, 1345. (t) Amiot, C. *J. Mol. Spectrosc.* **1980**, *81*, 424.

there are but two, RbH and CsH, for which the UICCs give higher errors than all of the other functions tested. For these molecules, the core–valence intershell correlation affects the PECs as strongly as, or even stronger than, the valence shell correlation.⁶⁵ The former effect has been successfully accounted for by core polarization potentials (CPP),^{65,66} which we are about to incorporate into our model.⁶⁷ In addition, the ground-state X $^1\Sigma^+$ of the alkali metal hydrides significantly interacts with the

excited A $^1\Sigma^+$ state from relatively low vibrational states on, e.g., NaH beyond $v = 9$.⁵⁴

Hydrides bearing a positive partial charge on H are well described by our UICCs. The relative differences of the PECs for the OH radical are displayed in Figure 9. While the Morse and Rydberg curves fail badly even close to R_e , the UIC deviations average to about 0.6% of D_e for more than 75% of the curve's energy range. The performance of the UIC curve is

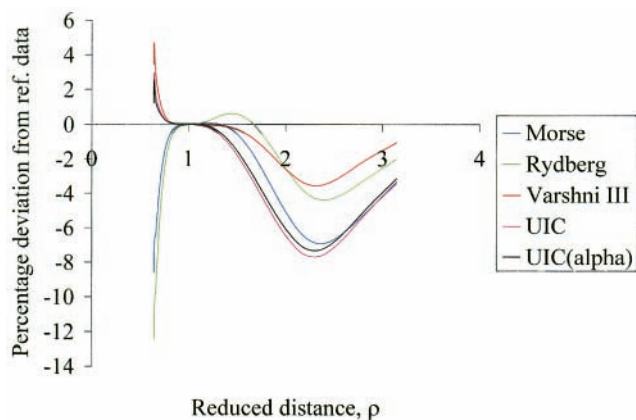


Figure 8. Lithium hydride ($Q_{\text{Li}} = 0.473$): relative potential energy difference ($U_{\text{cal}} - U_{\text{ref}}/D_e$) over reduced distance, R/R_e , shown for the UIC $_{\alpha}$ (black), UIC (pink), Varshni III (red), Rydberg (green), and Morse (blue) PECs. RKR reference data from: Vidal, C. R.; Stwalley, W. J. *Chem. Phys.* **1982**, *77*, 883.

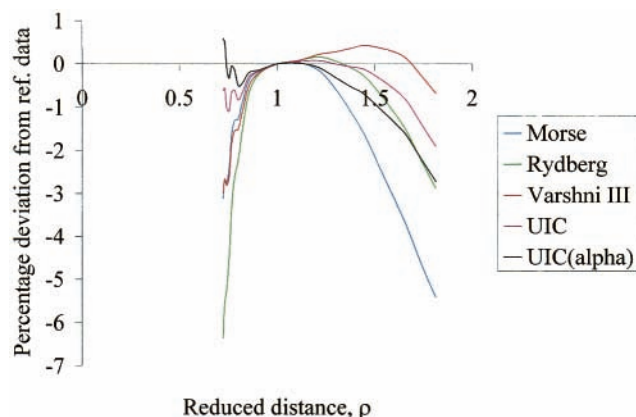


Figure 9. Hydroxyl radical ($Q_{\text{H}} = 0.298$): relative potential energy difference ($U_{\text{cal}} - U_{\text{ref}}/D_e$) over reduced distance, R/R_e , shown for the UIC $_{\alpha}$ (black), UIC (pink), Varshni III (red), Rydberg (green), and Morse (blue) PECs. Ab initio reference data from: Meyer, W.; Rosmus, P. J. *Chem. Phys.* **1975**, *63*, 2356.

twice as good as that of Varshni III and nearly 4 times better than those of Rydberg and Morse. The closeness between D_{vs} and $D_{\text{vs}}^{(\omega)}$ is evidence of good representation of the PEC for OH by the UIC function. The same holds for SH and would be expected for other group 16 hydrogen-containing diatoms, e.g., SeH.

For HCl, the use of 14.4% s-character instead of an earlier 10% significantly reduces the associated error from 3.89% to 1.57% for the UIC and 1.26% for the UIC $_{\alpha}$ function. The trend in deviation from RKR of VSM and UIC curves for the various molecules closely parallels that obtained for the VS function in the repulsive branch of the PEC.¹ Consequently, the accounts for anomalous molecules are similar. Following up on the discussion on O₂ in its $^3\Sigma_g$ ground state (section 4), we note that both UIC and UIC $_{\alpha}$ yield a low value of about 0.75% average unsigned error. This is remarkable, since the O₂ triplet ground state PEC has been considered difficult to model.^{4,33}

Overall, the comparison of all the calculated PECs with the corresponding RKR or ab initio data sets gives average unsigned errors of 1.42% and 1.16% for the $[R_e, k_e, D_{\text{vs}}, D_e, Q]$ UIC and the operational $[R_e, k_e, \alpha_c, D_e, Q]$ UIC $_{\alpha}$ functions, respectively. These are compared with the errors obtained for the three-parameter Morse,²⁴ Rydberg,⁹ and Varshni III¹¹ PECs. For the given set of bonds, the Varshni III function has an average

unsigned error of 2.76%, which is more than 1% higher than the corresponding error in the UIC functions, but is clearly less than that of other three-parameter functions. Relying on Nalewajski's statement²³ that none of Varshni's PECs approached $+\infty$ for $R \rightarrow 0$, we first missed¹ an exception, i.e., that the Varshni III potential does indeed reach the required positive infinity at $R = 0$. According to our experience,¹ this may contribute to its improved performance. On the other hand, the prediction of the anharmonicity constant has been shown to be exceptionally poor for the Varshni III PEC.¹² The Morse function displays an overall error of 3.92%, i.e., more than twice that of either of the UICs. Averaged over the whole set of 42 diatoms, the UICs are the only functions showing average unsigned deviations of less than 2% from the RKR data. According to the conclusions reached by Steele, Lippincott, and Vanderslice,¹² "the better 5-parameter functions should give average error of 1 to 2%." Notable examples of molecules for which the average unsigned error of both UICs falls significantly below the 1% barrier are H₂, N₂, O₂, Br₂, ICl, OH, and NO. The overall performance of both our PECs comes close to the optimum 1%, while our number of parameters per molecule is four (for homonuclear) to five (for polar bonds). We have evaluated the average unsigned error $\delta U/D_e$ using Murrell and Sorbie's five-parameter extended Rydberg PEC¹³ for 39 diatoms and get an overall 1.39%, the largest deviations being 4.1% for LiF, 5.1% for NaF, and 9.8% for NaCl. The latter errors are on average 4.5 times those of the UICs and add to the strong evidence³³ that the exponential PEC ansatz is inadequate for highly ionic bonds. Although we do not break the error barrier of 1% of D_e for as many molecules as Zavitsas,³³ we obtain high-quality calculated PECs for alkali metal halides, for which his model completely breaks down.^{33,68} In this sense, our model is closer to being universal.

5. Summary and Outlook

We have extended the validity range of the valence-state potential curve¹ (VS PEC) beyond the Coulson–Fischer transition² and up to $R \rightarrow \infty$. Universality of the PEC has been achieved by modeling a "soft" Coulson–Fischer transition by a continuous reduction of the weight of "ionic structures" in a composite potential function. Thereby the asymptotic reference energy is monotonically shifted from that of the promoted valence-state atoms (VSA) to that of the ground-state atoms. For the set of 42 diatomic molecules (from H₂ to NaCl), our UIC $_{\alpha}$ PEC yields an average unsigned error of 1.16% of D_e , which is a result near the optimum obtainable with five-parameter PECs.

Work is in progress to present more advantages of our semiempirical PECs by evidencing:

- (i) Their intrinsic potential for methodical development through improvements of the underlying physical model, e. g., by the inclusion of core-polarizability;⁶⁷
- (ii) The additivity and/or transferability of several parameters,⁶⁹ in addition to the one already reported,⁶ viz., the scaled force constant $\lambda = k_e R_e / D_{\text{vs}}$;
- (iii) The universal scaling properties of the UIC–PECs.⁷⁰

Acknowledgment. We acknowledge the significant contributions of Prof. Frantisek Jenč, Universität Marburg, by providing tables of RKR and ab initio data for most of the molecules examined and for discussions. We thank Dr. Willem Mulder and Dr. Ratna Ghosh for their useful comments and suggestions. L.v. Sz. thanks Prof. Hans-Joachim Werner, Universität Stuttgart, for his hospitality during the academic year 1999/2000. The work was presented, in part, at the Third

Conference of the International Society for Theoretical Chemical Physics, México D.F., México, November 1999.

References and Notes

- (1) Gardner, D.; Szentpály, L. v. *J. Phys. Chem. A* **1999**, *103*, 9313.
- (2) (a) Coulson, C. A.; Fischer, I. H. *Philos. Mag.* **1949**, *40*, 386. (b) Senatore, G.; March, N. H. *Rev. Mod. Phys.* **1994**, *66*, 445–474. (c) Gerratt, J.; Cooper, D. L.; Karadakov, P. B.; Raimondi, M. *Chem. Soc. Rev.* **1997**, *26*, 87.
- (3) (a) Szentpály, L. v. *J. Mol. Struct. (THEOCHEM)* **1991**, *233*, 71. (b) Szentpály, L. v.; Shamovsky, I. L. *J. Mol. Struct. (THEOCHEM)* **1994**, *305*, 249.
- (4) Szentpály, L. v. *Chem. Phys. Lett.* **1995**, *245*, 209.
- (5) Freeman, G.; March, N. H.; Szentpály, L. v. *J. Mol. Struct. (THEOCHEM)* **1997**, *394*, 11.
- (6) Szentpály, L. v. *J. Phys. Chem. A* **1998**, *102*, 10912.
- (7) Parr, R. G.; Szentpály, L. v.; Liu, S. J. *Am. Chem. Soc.* **1999**, *121*, 1922.
- (8) Szentpály, L. v. *Int. J. Quantum Chem. "Ruedenberg Festschrift."* **2000**, *76*, 222.
- (9) Rydberg, R. Z. *Phys.* **1931**, *73*, 376; *Z. Phys.* **1933**, *80*, 514.
- (10) (a) Klein, O. Z. *Phys.* **1932**, *76*, 221. (b) Rees, A. L. G. *Proc. Phys. Soc. (London)* **1947**, *59*, 998.
- (11) Varshni, Y. P. *Rev. Mod. Phys.* **1957**, *29*, 664.
- (12) Steele, D.; Lippincott, E. R.; Vanderslice, J. T. *Rev. Mod. Phys.* **1962**, *34*, 239.
- (13) (a) Murrell, J. N.; Sorbie, K. S. *J. Chem. Soc., Faraday Trans. 2* **1974**, *70*, 1552. (b) Huxley, P.; Murrell, J. N. *J. Chem. Soc., Faraday Trans. 2* **1983**, *79*, 323. (c) Sun, W.; Fen, H. *J. Phys. B* **1999**, *32*, 5109.
- (14) Dunham, J. L. *Phys. Rev.* **1932**, *41*, 713, 721.
- (15) Simons, G.; Parr, R. G.; Finlan, J. M. *J. Chem. Phys.* **1973**, *59*, 3229.
- (16) Ogilvie, J. F. *Proc. R. Soc. London, Ser. A* **1981**, *A378*, 287.
- (17) Molski, M. *Phys. Rev. A* **1999**, *60*, 3300.
- (18) Jordan, K.; Kinsley, J. L.; Silbey, R. J. *Chem. Phys.* **1974**, *61*, 911.
- (19) (a) Wales, D. J. *Science* **1996**, *271*, 925. (b) Hartke, D. J. *Comput. Chem.* **1999**, *20*, 1752.
- (20) Rittner, E. S. *J. Chem. Phys.* **1951**, *19*, 1030.
- (21) Varshni, Y. P.; Shukla, R. C. *Rev. Mod. Phys.* **1963**, *35*, 130.
- (22) Borkman, R. F.; Parr, R. G. *J. Chem. Phys.* **1968**, *48*, 1116.
- (23) Nalewajski, R. J. *Phys. Chem.* **1978**, *82*, 1439.
- (24) Morse, P. M. *Phys. Rev.* **1929**, *34*, 57.
- (25) Brenner, D. W. *Phys. Status Solidi B* **2000**, *217*, 23.
- (26) Frost, A. A.; Musulin, B. J. *Am. Chem. Soc.* **1954**, *76*, 2045.
- (27) (a) Jenč, F. *Adv. At. Mol. Phys.* **1983**, *19*, 265. (b) Jenč, F. *Phys. Rev. A* **1990**, *42*, 403. (c) Jenč, F. *Int. Rev. Phys. Chem.* **1996**, *15*, 467.
- (28) (a) Ferrante, J.; Smith, J. R.; Rose, J. H. *Phys. Rev. Lett.* **1983**, *50*, 1383. (b) Rose, J. H.; Smith, J. R.; Ferrante, J. *Phys. Rev. B* **1983**, *28*, 1835. (c) Smith, J. R.; Schlosser, H.; Leaf, W.; Ferrante, J.; Rose, J. H. *Phys. Rev. A* **1989**, *39*, 514.
- (29) (a) Graves, J. L.; Parr, R. G. *Phys. Rev. A* **1985**, *31*, 1. (b) Graves, J. *Int. J. Quantum Chem.* **1997**, *65*, 1.
- (30) Tellinghuisen, J.; Henderson, S. D.; Austin, D.; Lawley, K. P.; Donovan, R. J. *Phys. Rev. A* **1989**, *39*, 925.
- (31) (a) Jhung, K. S.; Kim, I. H.; Hahn, K. B.; Oh, K.-H. *Phys. Rev. A* **1989**, *40*, 7409. (b) Jhung, K. S.; Kim, I. H.; Oh, K.-H.; Hahn, K. B. *Phys. Rev. A* **1990**, *42*, 64.
- (32) Wei Hua, *Phys. Rev. A* **1990**, *42*, 2524.
- (33) Zavitsas, A. A. *J. Am. Chem. Soc.* **1991**, *113*, 4755.
- (34) (a) Van Hooydonk, G. Z. *Naturforsch.* **1982**, *37a*, 710, 971. (b) Van Hooydonk, G., *Eur. J. Inorg. Chem.* **1999**, 1617.
- (35) Ruedenberg, K. *Rev. Mod. Phys.* **1962**, *34*, 326.
- (36) Slater, J. C. *Quantum Theory of Molecules and Solids*; McGraw-Hill: New York, 1963; Vol. 1, Sections 4-5 and 7-3.
- (37) Harris, F. E.; Pohl, H. A. *J. Chem. Phys.* **1963**, *42*, 3648.
- (38) March, N. H. Private communication.
- (39) (a) Gunnarson, O. B.; Lundquist, B. I. *Phys. Rev. B* **1976**, *13*, 4274. (b) Pettifor, D. G. *Bonding and Structure of Molecules and Solids*; Clarendon, Oxford, UK, 1995; p 60 ff.
- (40) Teter, M. *Phys. Rev. B* **1993**, *48*, 5031.
- (41) Smith, R. P.; Ree, T. K.; Magee, J. L.; Eyring, H. *J. Am. Chem. Soc.* **1951**, *73*, 2263.
- (42) (a) Bergmann, D.; Hinze, J. *Struct. Bonding (Berlin)* **1987**, *61*, 145. (b) Bergmann, D.; Hinze, J. *Angew. Chem.* **1996**, *108*, 162; *Angew. Chem., Int. Ed. Engl.* **1996**, *35*, 150.
- (43) Rappé, A. K.; Goddard, W. A. *J. Phys. Chem.* **1991**, *95*, 3358.
- (44) Itskowitz, P.; Berkowitz, M. L. *J. Phys. Chem. A* **1998**, *102*, 4808.
- (45) Rodrigues, R.; Szentpály, L. v. Unpublished results.
- (46) Bratsch, S. G. *J. Chem. Educ.* **1988**, *65*, 34.
- (47) Werner H.-J.; Meyer, W. *J. Chem. Phys.* **1981**, *74*, 5802.
- (48) The Morse function has been used in different reparametrized and modified forms by Nalewajski²³ and Tellinghuisen [Tellinghuisen, J. (a) *Chem. Phys. Lett.* **1982**, *91*, 447; (b) *Can. J. Chem.* **1989**, *67*, 820]. These reparametrizations have altered the value of the Sutherland parameter or $a = \Delta^{1/2}$ in order to refine the curvature around the potential minimum by reproducing experimental α_e and/or ν_{e_c} values. In consequence, the function does not correctly dissociate into ground-state atoms; for a recent discussion, see ref 1. We wish to enforce the proper dissociation and, therefore, need the input of the experimental D_e .
- (49) Dewar, M. J. S. *The MO Theory of Organic Chemistry*; McGraw-Hill: New York, 1969; p 448.
- (50) Szentpály, L. v. *Theor. Chim. Acta (Berlin)* **1979**, *52*, 277.
- (51) (a) Amiot, C.; Crozet, P.; Vergès, J. *Chem. Phys. Lett.* **1985**, *121*, 390. (b) Seto, J. Y.; Le Roy, R. J.; Vergès, J.; Amiot, C. *J. Chem. Phys.* **2000**, *113*, 3067.
- (52) Focsa, C.; Li, H.; Bernath, P. F. *J. Mol. Spectrosc.* **2000**, *200*, 104.
- (53) Brand, J. C. D.; Hoy, A. R. *J. Mol. Spectrosc.* **1985**, *114*, 197.
- (54) Pesl, F. P.; Lutz, S.; Bergmann, K. *Eur. Phys. J. D* **2000**, *10*, 247.
- (55) Driessler, F.; Kutzelnigg, W. *Theor. Chim. Acta* **1977**, *43*, 1, 307.
- (56) Peters, D. *J. Chem. Soc.* **1963**, 2003, 2015.
- (57) (a) Sanderson, R. T. *Chemical Bonds and Bond Energy*; Academic Press: New York, 1976; p 10. (b) Sanderson, R. T. *Polar Covalence*; Academic Press: New York, 1983.
- (58) *CRC Handbook of Chemistry and Physics*, 100th ed.; Lide, D. R., Ed.; CRC Press: Boca Raton, FL, 2000.
- (59) The experimental F values are obtained from the α_e , B_e , and $\tilde{\nu}_e$ compiled in: (a) Huber, K. P.; Herzberg, G. *Molecular Spectra and Molecular Structure IV: Constants of Diatomic Molecules*; Van Nostrand Reinhold: New York, 1979. (b) Landolt-Börnstein. *Numerical Data and Functional Relationships in Science and Technology, New Series II/61974, II14a1982, II14b1983, II19a1992, II19d-11995: Molecular Constants*; Springer-Verlag: Heidelberg, 1974–1995.
- (60) For our purpose, the term "unsigned error" is much preferable to "absolute error". The latter is frequently used in two confusing connotations: unambiguously, as opposed to "relative error", but also as error modulus ("unsigned error") which itself is of either the absolute or relative type.
- (61) Konowalow, D. D.; Olson, M. L. *J. Chem. Phys.* **1979**, *71*, 450.
- (62) Swaminathan, P. K.; Clementi, E. *J. Phys. Chem.* **1987**, *91*, 1020.
- (63) Swaminathan, P. K.; Laaksonen, A.; Corongiu, G.; Clementi, E. *J. Chem. Phys.* **1986**, *84*, 867.
- (64) Meyer, W.; Rosmus, P. *J. Chem. Phys.* **1975**, *63*, 2356; *J. Chem. Phys.* **1976**, *65*, 492.
- (65) (a) Fuentealba, P.; Preuss, H.; Stoll, H.; Szentpály, L. v. *Chem. Phys. Lett.* **1982**, *89*, 418. (b) Szentpály, L. v. *Chem. Phys. Lett.* **1982**, *88*, 321. (c) Szentpály, L. v.; Fuentealba, P.; Preuss, H.; Stoll, H. *Chem. Phys. Lett.* **1982**, *93*, 555.
- (66) (a) Müller, W.; Flesch, J.; Meyer, W. *J. Chem. Phys.* **1984**, *80*, 3297. (b) Müller, W.; Meyer, W. *J. Chem. Phys.* **1984**, *80*, 3311.
- (67) Donald, K.; Mulder, W.; Szentpály, L. v. Unpublished results.
- (68) Further molecules for which the Zavitsas PEC breaks down and cannot be applied are AlF, SrF, BaF, LaO, and ThO, while BF, GaF, and GaCl are on the borderline.
- (69) Szentpály, L. v. Ghosh, R. Unpublished results.
- (70) Gardner, D.; Szentpály, L. v. Unpublished results.